Structural Characteristics of Pedestrian Slab Bridge Using GFRP Pultrusion Profiles

Xian Cui *, Ken-ichi Maeda **, Hitoshi Nakamura ***, Nobuhiko Kitayama ****, Tetsuya Watanabe *****

* Master's course, Dept. of Civil and Environmental Eng., Tokyo Metropolitan University, 1-1, Minami-Osawa, Hichioji City, Tokyo 192-0397
** Dr. of Eng., Professor, Dept. of Civil and Environmental Eng., Tokyo Metropolitan University, 1-1, Minami-Osawa, Hichioji City, Tokyo 192-0397
*** M. of Eng., Research Associate, Dept. of Civil and Environmental Eng., Tokyo Metropolitan University, 1-1, Minami-Osawa, Hichioji City, Tokyo 192-0397
**** Bridge Dept., Ishikawa-Harima Heavy Industries Co., Ltd, 3-2-16, Toyosu, Koto-Ku, Tokyo 135-8733
***** C&A Dept., Asahi Glass Matex Co., Ltd, 1-2-27, Miyashita, Sagamihara City, Kanagawa 229-1112

Fiber reinforced plastic (FRP) has drawn attention as a new construction material recently. This paper dealt with development of a newly proposed pedestrian slab bridge using GFRP pultrusion profiles reinforced with glass fibers. In this study, after material tests were done in order to grasp material properties of two kinds of GFRP pultrusion profiles, a trial design of this new pedestrian bridge was performed based on the properties. Next, bending load tests and falling vibration tests using a specimen of real size were done, and analytical examination was also carried out in order to investigate the static and dynamic bending deformation characteristics of the specimen and of the trial design bridge. Moreover, from these results, it was proven that the possibility of practical application of this new bridge is very high.

Key Words: Glass fiber reinforced Plastic, Pultrusion profile, Pedestrian bridge, Slab bridge, Deflection limitation, Vibration serviceability

1. Introduction

While the importance of rationalization of the construction work and the maintenance in civil engineering structures is pointed out in recent years, fiber-reinforced plastic (FRP) has become to attract attention as new structural materials. Much research and development of pedestrian bridges or highway bridges made from FRP structural members have already been carried out energetically in the world [1), 2)].

In Particular, pedestrian bridges made of all glass fiber reinforced plastics (GFRPs) have raised many results steadily in the world. Since the gravity is ultra light at about 2.0 or less, the workability is excellent, and the rapid construction becomes possible. The adaptability to a very disadvantageous area in respect of environmental condition is also excellent, such as damage from salt or acid, and the control of maintenance becomes rational.

In Japan, the Ikei-Tairagawa Road Park Bridge made of all GFRPs was completed to Okinawa Prefecture for the first time as a practical bridge in March 2000 [3)]. This pedestrian bridge is a two spans continuous plate-girder bridge with the length of about 38m and the width of 3.5m. However, since materials molded by the hand lay-up were used for the main girder, even if the life cycle cost were estimated, it left the subject in respect of cost. Therefore, it is indispensable to establish the design method what can sharply reduce the material cost.

In the case of a pedestrian bridge, pultrusion profiles are applicable enough, and drastic reduction of the material cost is attained. This is because it became possible to be able to manufacture large-sized cross-section profiles by the pultrusion molding, and to use as a member for the main girder of a pedestrian bridge.

From such a viewpoint, this study dealt with the development of a newly proposed pedestrian slab bridge using GFRP pultrusion profiles bonded together by adhesives [4), 5)].

First, material tests were done in order to grasp material properties of two kinds of GFRP pultrusion profiles. Next, based on the material properties, a trial design of this new pedestrian bridge was performed. Then, a specimen of real size was made, and bending load tests and falling vibration tests were done. Furthermore, analytical examination is carried out in order to investigate the static and dynamic bending deformation characteristics of the specimen and of the trial design bridge, by comparing with the test results.

2. Material Properties of GFRP Pultrusion Profiles

This newly proposed pedestrian slab bridge has adopted the tallest GFRP profile called I300 and the wide one called F1000 in those days. Material arrangement of I300 and F1000 is shown in Fig.1. The reinforcement fiber is the e-glass fiber, and the polymer matrix is the unsaturated polyester resin

Material tests were done based on JIS. The tension test, the compression test and the shear test were carried out using the tension and compression load testing machine with capacity of 100kN as shown in Fig.2 (a). Moreover, the bending test was carried out using the bending load equipment with capacity of 10kN as shown in Fig.2 (b). For the shear test, the jig shown in Fig.2 (c) was used as the basis of JIS.

Typical material properties evaluated by the test results are shown in Table 1. Since the arrangement of each part differs, the material properties are different in each part. Moreover, the properties are different in the same part by each direction.

In comparing with the elastic modulus and the tension strength in case of one sheet of F1000, these values in case of two sheets decrease by being bonded together using an adhesive layer. Though the elastic modulus and the tension strength of this adhesive layer are the values shown in Table 1, the shear strength was quite small at 4.6MPa. Therefore, on designing, it is necessary to be adequately considered that shear fracture at a bonded part may become dominant.

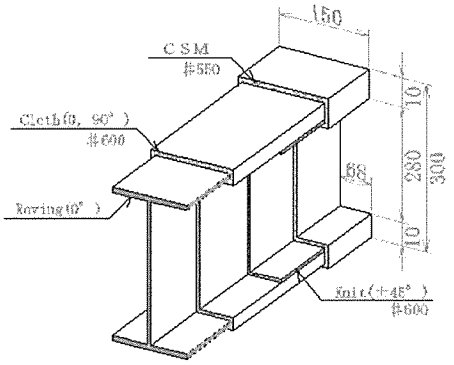

(a) I300

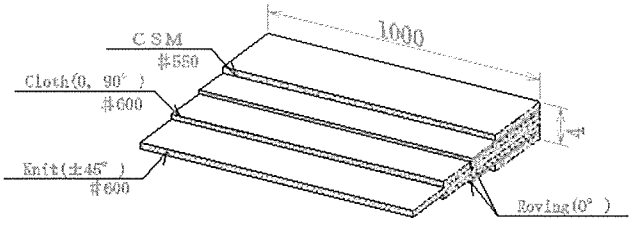

(b) F1000

Fig.1 Arrangement of pultrusion profiles

Table 1 Material properties of pultrusion profiles

Material Property		Tension Elastic Modulus (GPa)	Tension Strength (MPa)
I300	Flange	32.2	406.8
	Web	25.4	Over 350
F1000	One sheet	29.1	409.0
	Two-sheets adhesion	21.8	333.2
Adhesive layer (with CM)		9.1	151.9

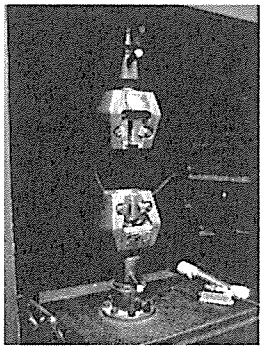

(a) For tension, compression and shear tests

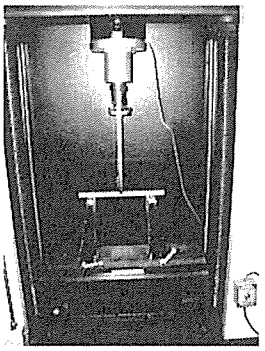

(b) For bending tests

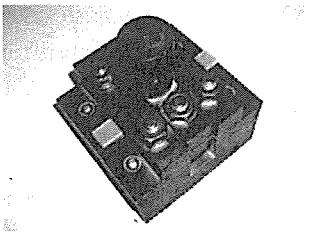

(c) The jig for shear tests

Fig.2 Testing method

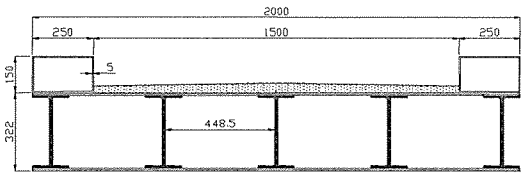

Fig.3 Sectional view of trial design bridge

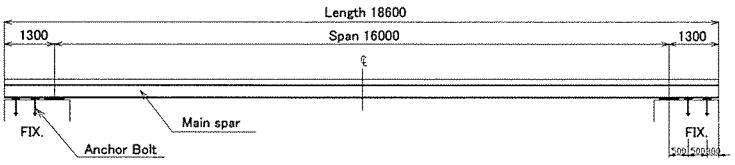

Fig.4 Side view and semi-fixed support condition

3. Trial Design of a GFRP Pedestrian Slab Bridge

In order to examine the possibility of practical application the newly proposed pedestrian slab bridge, the following trial design was performed in making the effective span and width to be 16m and 1.5m, respectively. All the components except mortar pavement used GFRP pultrusion profiles of which the material properties were made into the value acquired from material testing shown in Chapt.2.

The deck and bottom plates are the above-mentioned two sheets of F1000 bonded together by the adhesive layer, and are unified with five pieces of I300 by the different adhesive at a factory. Consequently, the unified section is made the resistance section to bending as shown in Fig.3.

Since the elastic modulus of GFRP is very low, the bending deflection was quite large in case of simple support conditions. Therefore, the authors should propose semi-fixed support conditions using anchor bolts at both ends. The side view is shown in Fig.4.

The dead load per bridge of the resistance section, the felloe guard, the railing and the pavement were 1.306kN/m, 0.125kN/m, 0.560kN/m and 1.202kN/m, respectively. The live load and the temperature change were made respectively to be 3.5kN/m^2 and ±30℃ with the Japanese standard for pedestrian bridges and underpasses drawn in 1979.

This standard has been determined that the allowable limiting value of the static deflection due to the live load should be made to be L/600, in which L is the effective span length, considering the serviceability.

In order to simplify the design, analytical calculation was performed by using a beam model perfectly fixed at both ends. As a result, the maximum stress was 19.81MPa, and the value greatly fell below the measured value of the tension strength. The maximum deflection of the central point was 23.10mm, and was slightly smaller than L/600 (L= 16m). These facts showed that the deflection limitation became dominant in the cross section decision. Therefore, it is indispensable to investigate the bending deformation characteristics correctly.

In addition, the aforesaid Japanese standard for pedestrian bridges has been determined that the natural frequency should avoid the zone of 1.5Hz to 2.3Hz considering the vibration serviceability. Therefore, it is also indispensable to investigate the bending vibration characteristics correctly.

4. Bending Deformation Characteristics and Calculation Methods of Deflection

4.1 Bending Load Test of Specimen

A specimen of real size was made as a partial model of the trial design bridge, and the four-points bending load tests were carried out. The side view at the time of setup of the specimen is shown in Fig.5, and the sectional view is shown in Fig.6. The situation photograph at the time of setup is shown in Fig.7.

The cross section of specimen consists of two I300 and two sheets of F1000 bonded together by the adhesive layer of 2mm thickness, as shown in Fig.6. Moreover, F1000 was being cut off on the center location of I300, and the adhesive was injected into the gap. Because, since the width of F1000 pultruded in a factory is 1000mm naturally, it is necessary to arrange them in actual bridges.

Load P was increased to 300kN by the load control, and the bending tests was carried out by the especially attention to

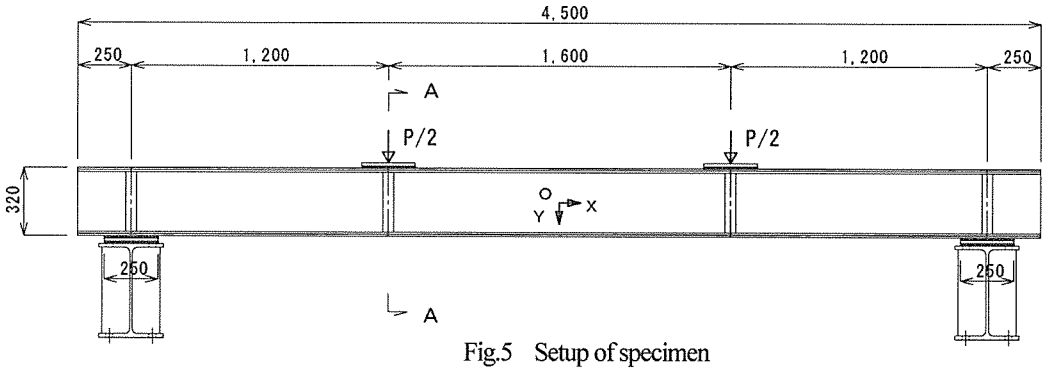

Fig.5 Setup of specimen

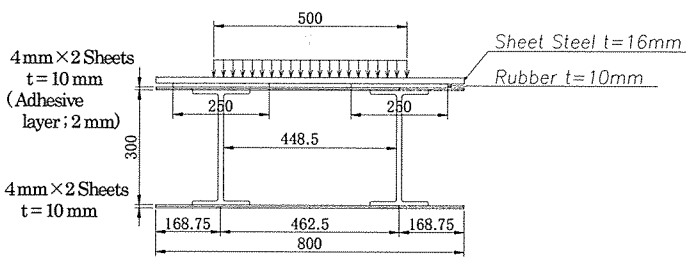

Fig.6 Cross section of specimen

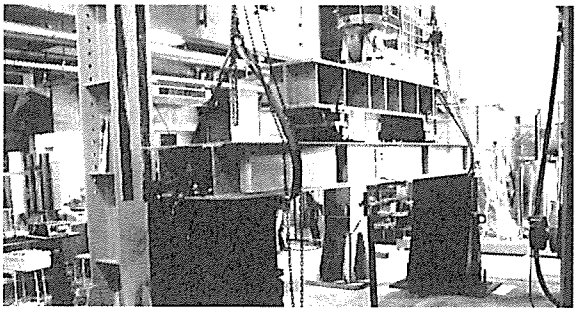

Fig.7 Situation of bending load test

deflection at the effective span center and the Bernoulli-Euler theory in which the cross section is always a plane.

Furthermore, in order to contrast with the test result, three kinds of computer analyses were done, and the physical properties were applied as shown in Table 2. Namely, the first method is the three-dimensional FEM analysis (MARC 2001) using solid elements and considering the orthotropy. The second is the framed structure analysis (Y-FIBER 3D) using fiber elements based on the Timoshenko beam theory which can consider effects of the shear deformation, and the third is the usual framed analysis based on Bernoulli-Euler beam theory.

Here, it is called for short "3D FEM", "Timo.Th." and "B.-E.Th.". By B.-E.Th., comparison examination was carried out about two cases, at the time that flexural rigidity of the adhesive layer of 2mm thickness is considered and at the time of not considering. Based on the material test results, the calculated flexural rigidity EI of the cross section was 1.55×10^7kN-m^2 in the former case. Then, in the latter case, it was 1.47×10^7kN-m^2.

Fig.8 shows comparison of the maximum deflection at the central point L/2 of the effective span L (=4.0m) at the time of the load P = 300 kN. Comparing to the experimental value, this figure shows that the deflection is small evaluated about 6 to 10% by B-E Th.. Moreover, in 3D FEM and Timo.Th., it is proven to agree with the experimental value. Because the difference of 3D FEM and Timo.Th. is slight, it seems that the influence due to the anisotropy of material on the bending deformation characteristics is very small.

The distribution of normal strain in the cross section at the central point L/2 and of normal stress distribution are shown in Fig.9 and Fig.10. From these figures, it is confirmed that the cross section has satisfied the assumption of the Bernoulli-Euler theory. Moreover, with the rise of the analysis level, it can be said that it would be able to more faithfully reproduce the experimental result.

4.2 Analytical Examination of Trial Design Bridge

Continuously, by the above-mentioned three kinds of analysis methods, analytical examination about the bending deformation characteristics was performed for the trial design bridge. Since this bridge was proposed to have semi-fixed support conditions at both ends, examination in case of perfectly fixed support conditions was also carried out by B.-E.Th.. for the comparison.

Fig.11 shows comparison of the deflection distribution by each analysis method, when fully loading of the live load in the effective span. First, from this figure, it is confirmed that the difference of the semi-fix and the perfect fix is not great, and that anchor bolts have placed effectively.

Also, because the maximum deflection by 3D FEM and Tim.Th. is about 10% bigger than the one by B.-E.Th. when the adhesive layer was disregarded, it is proven that effects of the shear deformation on the bending deformation characteristics cannot be disregarded. Moreover, since the difference is further expanded when consideration of the adhesive layer, it can be

Table.2 Physical properties of material

		F1000	I300		Adhesive Layer
			Flange	Web	
Young's modulus (GPa)	E_X	29.1	34.2	25.4	9.1
	E_Y	(3.0)	(3.0)	11.4	
	E_Z	10.3	15.1	(3.0)	
Poisson's ratio	ν_{XY}	(0.30)	(0.30)	0.44	(0.30)
	ν_{YZ}	(0.30)	(0.30)	(0.30)	
	ν_{ZX}	(0.30)	0.35	(0.30)	
Shear modulus (GPa)	G_{XY}	(2.0)	(2.0)	4.1	(3.5)
	G_{YZ}	(2.0)	(2.0)	(2.0)	
	G_{ZX}	4.5	(4.0)	(2.0)	
Tensile Strength(MPa)		409.0	406.8	(Over 350)	151.9
Density (kN/m^3)		17.99	17.55	17.55	13.01

X:Longitudinal drientation Y:Transverse direction
Z:Vertical direction *( )Inside is an assumed value.

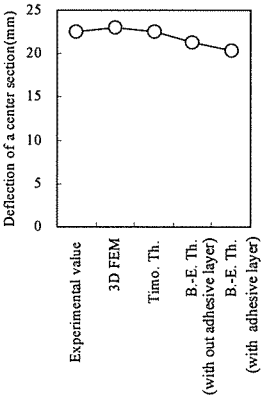

Fig.8 Comparison of deflection

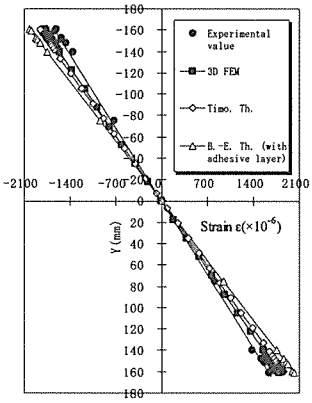

Fig.9 Normal strain distribution

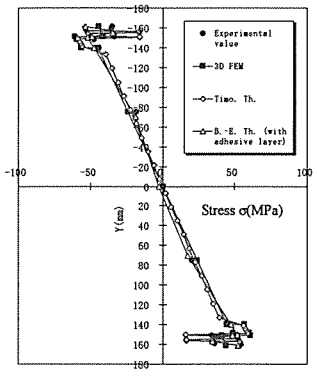

Fig.10 Normal stress distribution

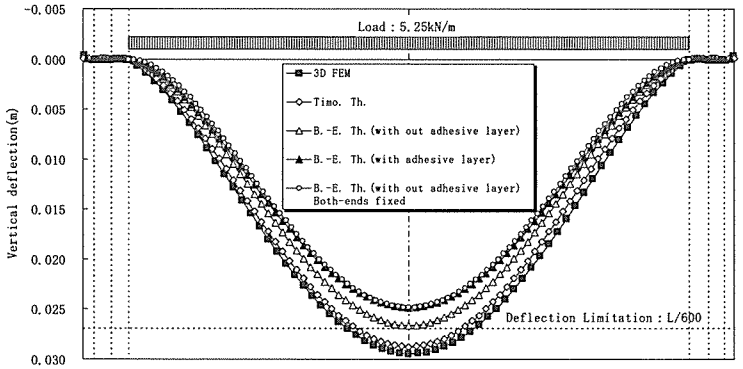

Fig.11 Comparison of deflection of trial design bridge

said that it needs to be appropriately evaluated about the adhesive layer. Then, as a result of calculating in consideration of the deflection accompanying the shear deformation for the cross sectional configuration of this bridge, applicable effective span length was exactly set to 15.363m.

5. Bending Vibration Characteristics and Estimation of Vibration Serviceability

5.1 Falling Vibration Test of Specimen

Using the test specimen made for the bending load test, acceleration sensors were installed in L/2 point and L/4 point, and the falling vibration test was done by jumping down of a man as shown in Fig.16. Moreover, three kinds of analysis methods were applied like the bending load test.

Fig.12 shows the measured acceleration waveform, and Fig.13 shows the spectral analysis diagram by FFT. As a result, the first symmetric deflection natural frequency was 27.34Hz. Fig.14 shows comparison of this measured value and the analytic value by each analysis method. From this figure, it is proven that the difference of these values tends to be completely similar to the case of the bending load test.

Furthermore, in order to grasp damping properties, the acceleration waveform after adjustment by a low pass filter of

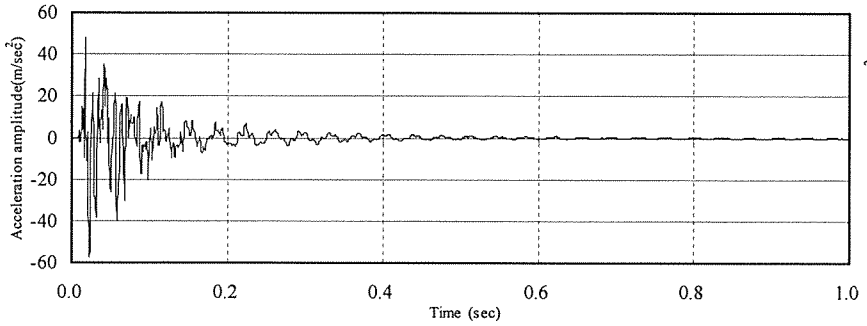

Fig.12 Acceleration waveform in L/2 point

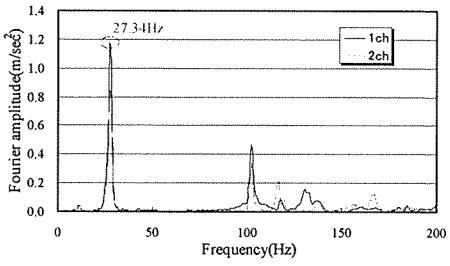

Fig.13 FFT analysis diagram

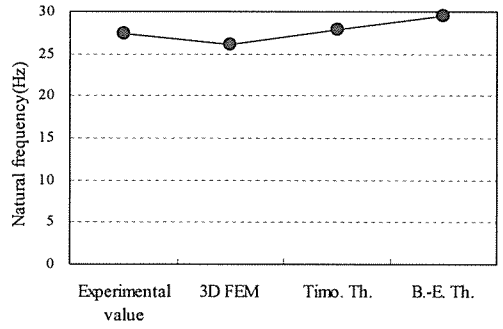

Fig.14 Comparison of measured and analytic values

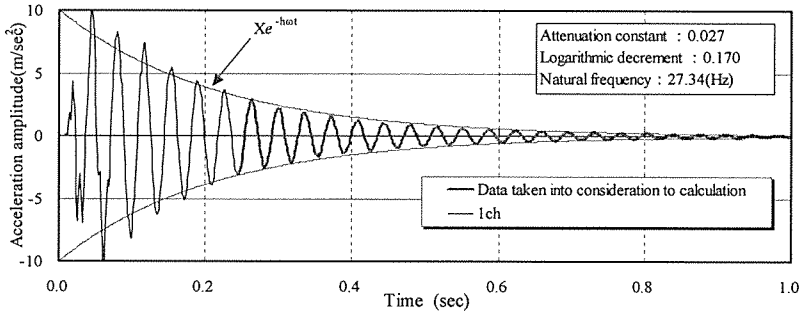

Fig.15 Waveform after adjustment with a low pass filter

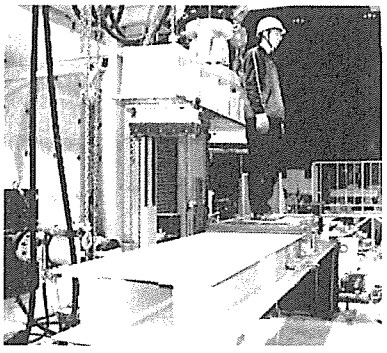

Fig.16 Falling vibration test

Table.3 Vibration modes and natural frequencies of trial design bridge

Analysis method	Mode of vibration	Natural frequency (Hz)
3D FEM	The first symmetric deflection mode	3.86
	The first symmetric torsion mode	8.63
	The first antisymmetric deflection mode	10.31
	The second symmetric deflection mode	19.58
	The second symmetric torsion mode	25.02
	The second antisymmetric deflection mode	30.73
Timo. Th.	The first symmetric deflection mode	4.28
	The first antisymmetric deflection mode	11.70
	The second symmetric deflection mode	22.61
	The second antisymmetric deflection mode	36.66
B.-E. Th.	The first symmetric deflection mode	4.63
	The first antisymmetric deflection mode	12.78
	The second symmetric deflection mode	25.08
	The second antisymmetric deflection mode	41.49

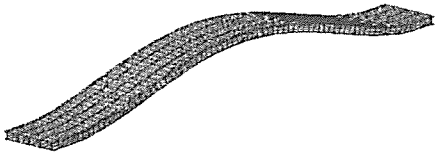

3.86Hz

(a) The first symmetric deflection mode

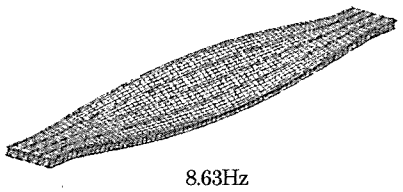

8.63Hz

(b) The first symmetric torsion mode

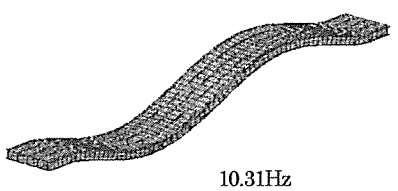

10.31Hz

(c) The first antisymmetric deflection mode

Fig.17 Vibration modes and natural frequencies by 3D FEM of trial design bridge

100Hz was described as shown in Fig.15. From this figure, the calculated value of the damping constant was 2.7%, and was very high. Hence, it is confirmed that the damping property of FRP is considerably higher than other general materials.

5.2 Analytical Examination of Trial Design Bridge

Continuously, by the above-mentioned three kinds of analysis methods, analytical examination about the bending vibration characteristics was performed for the trial design bridge which has semi-fixed support conditions at both ends.

Table 3 shows vibration modes and natural frequencies by each analysis method. Typical vibration modes and natural frequencies by 3D FEM are shown in Fig.17.

From these table and figure, since the natural frequency by 3D FEM becomes the lowest, the possibility to which the anisotropy of material affects is considered sufficiently. Moreover, because the natural frequency of the first symmetric deflection mode is higher than the resonance zone of 1.5Hz to 2.3Hz what should be avoided, it was confirmed that the vibration serviceability is satisfactory.

6. Conclusion

From the result of the material tests, the trial design, the bending load tests, the falling vibration tests and the analytical examination, described in until now chapter, it was proven that the possibility of practical application of this newly proposed pedestrian slab bridge using GFRP pultrusion profiles is very high. Furthermore, it was possible to sufficiently obtain the design data on the bending deformation and vibration characteristics, which influence the cross section decision and the static and dynamic serviceability.

References

1) T. Keller, et al. : Advanced Materials, Structural Engineering International, IABSE, Vol.9, No.4, pp.250-301, 1999.
2) T. Keller, et al. : Advanced Materials, Structural Engineering International, IABSE, Vol.12, No.2, pp.66-116, 2002.
3) Japan Society of Civil Engineers (JSCE): FRP Bridges - Technologies and their Future - (edited by K. Maeda), Structural Engineering Series 14, Maruzen, pp.182-191, Jan. 2004, (in Japanese).
4) K. Maeda, N. Kitayama, H. Nakamura, K. Hayashi, Y. Kajikawa : Vibration Serviceability of Pedestrian Slab Bridges Developed Using GFRP Pultrusion Members, Proc. of Colloquium on Bridge Vibration '03, JSCE, pp.283-287, Sept. 2003, (in Japanese).
5) K. Maeda, N. Kitayama, H. Nakamura, K. Hayashi, Y. Kajikawa : Serviceability of Pedestrian Bridges Developed Using GFRP Pultrusion Members, Journal of Structural Engineering, JSCE, Vol.50A, pp.375-382, Mar. 2004, (in Japanese).